Adjuvant effect of the novel TLR1/TLR2 agonist Diprovocim synergizes with anti–PD-L1 to eliminate melanoma in mice

Ying Wang[a], Lijing Su[a], Matthew D. Morin[b], Brian T. Jones[b], Yuto Mifune[b], Hexin Shi[a], Kuan-wen Wang[a], Xiaoming Zhan[a], Aijie Liu[a], Jianhui Wang[a], Xiaohong Li[a], Miao Tang[a], Sara Ludwig[a], Sara Hildebrand[a], Kejin Zhou[c,d], Daniel J. Siegwart[c,d], Eva Marie Y. Moresco[a], Hong Zhang[a], Dale L. Boger[b], and Bruce Beutler[a,1]

[a]Center for the Genetics of Host Defense, University of Texas Southwestern Medical Center, Dallas, TX 75390; [b]Department of Chemistry, The Scripps Research Institute, La Jolla, CA 92037; [c]Simmons Comprehensive Cancer Center, University of Texas Southwestern Medical Center, Dallas, TX 75390; and [d]Department of Biochemistry, University of Texas Southwestern Medical Center, Dallas, TX 75390

Edited by Dennis A. Carson, University of California, San Diego, La Jolla, CA, and approved July 2, 2018 (received for review June 28, 2018)

Successful cancer immunotherapy entails activation of innate immune receptors to promote dendritic cell (DC) maturation, antigen presentation, up-regulation of costimulatory molecules, and cytokine secretion, leading to activation of tumor antigen-specific cytotoxic T lymphocytes (CTLs). Here we screened a synthetic library of 100,000 compounds for innate immune activators using TNF production by THP-1 cells as a readout. We identified and optimized a potent human and mouse Toll-like receptor (TLR)1/TLR2 agonist, Diprovocim, which exhibited an EC_{50} of 110 pM in human THP-1 cells and 1.3 nM in primary mouse peritoneal macrophages. In mice, Diprovocim-adjuvanted ovalbumin immunization promoted antigen-specific humoral and CTL responses and synergized with anti–PD-L1 treatment to inhibit tumor growth, generating long-term antitumor memory, curing or prolonging survival of mice engrafted with the murine melanoma B16-OVA. Diprovocim induced greater frequencies of tumor-infiltrating leukocytes than alum, of which CD8 T cells were necessary for the antitumor effect of immunization plus anti–PD-L1 treatment.

TLR1/TLR2 | agonist | melanoma | PD-L1 antibody | cancer immunotherapy

By activating antigen presenting cells (APCs) including dendritic cells (DCs) and macrophages, adjuvants hold the potential to unleash the natural functions of cytotoxic T lymphocytes (CTLs) to kill pathogens or cancer. Many adjuvants including Toll-like receptor (TLR) agonists engage innate immune receptors on APCs, inducing APCs to present antigens, produce cytokines, and provide costimulatory signals (1, 2) to antigen-specific CD8 T cells. In response to these signals, CD8 T cells proliferate and differentiate into CTLs capable of killing infected or tumor cells expressing their target antigen. In addition, such signals activate CD4 T cells, inducing their expansion and differentiation into Th1 or Th2 T helper cells (3).

One of the most important targets of improved adjuvant technology lies in the field of cancer immunotherapy, where the adaptive immune system is exploited to kill cancer cells based on their expression of cancer-associated antigens or neoantigens (4, 5). The effectiveness of cancer immunotherapy depends on the generation and activation of tumor-specific CTLs (5, 6) and on their maintenance of activity in vivo, leading to killing of tumor cells and a long-lasting antitumor memory response (5). Thus, immune checkpoint inhibitors such as anti–PD-1, anti–PD-L1, and anti–CTLA-4 have achieved remarkable clinical success in the treatment of melanoma through their action in blocking pathways that inhibit CTL activation (7, 8). However, even among those tumors known to be susceptible to checkpoint blockade, response rates of only ∼20% have been reported for PD-1/PD-L1 antibody treatment (5, 9), possibly due to insufficient numbers or activation of tumor-reactive CTLs or their failure to infiltrate tumors. These deficiencies may be exacerbated by immunosuppression induced by the cancer environment.

TLR ligands have long been known to act as adjuvants in adaptive immune responses (10, 11) signaling via adapter proteins (MyD88, TRIF, TRAM, and MAL), kinases, and ubiquitin ligases to activate NF-κB and IRFs (12–14). These and other transcription factors induce the expression of thousands of genes that carry out the innate immune response (15). Several nucleotide-based adjuvants such as TLR3 agonist poly I:C (9), TLR9 agonist CpG (16), and STING agonist cGAMP (6) have been reported to improve the efficacy of immune checkpoint inhibitors in preclinical models for cancer treatment. These approaches aim to increase the number of tumor-specific CTLs upon which checkpoint inhibitors can act. However, they have relied chiefly on natural TLR ligands, which are difficult to synthesize and in some instances quite toxic, presumably because they become widely disseminated in vivo and activate myeloid cells indiscriminately, producing cytokine storm (17). We sought to develop agonists with superior pharmacologic properties, with defined structural and molecular mechanisms from which key adjuvant design principles may be learned.

By screening a library of synthetic compounds, we identified a potent human- and mouse-active TLR1/TLR2 agonist, Diprovocim, with no structural similarity to any microbial TLR agonist.

Significance

Adjuvants enhance adaptive immune responses, sometimes through unknown mechanisms, and can be used to augment both humoral and cellular responses to cancer antigens. We report the immunological effects of the synthetic chemical adjuvant Diprovocim, which targets the innate immune receptor TLR1/TLR2 in mice and humans. Diprovocim displayed strong adjuvant activity in mice, particularly abetting cellular immune responses. Immunization against a genetically engineered tumor-specific antigen, ovalbumin, when adjuvanted with Diprovocim, inhibited growth of B16 melanoma and prolonged survival in the presence of immune checkpoint blockade by anti–PD-L1; 100% of mice responded to treatment. Our data suggest Diprovocim boosts the success of anti–PD-L1 treatment by increasing the number and activation of tumor-specific CTLs capable of responding to this checkpoint inhibitor.

Author contributions: Y.W. and B.B. designed research; Y.W., L.S., H.S., K.-w.W., X.Z., A.L., J.W., X.L., M.T., S.L., S.H., K.Z., D.J.S., and H.Z. performed research; M.D.M., B.T.J., Y.M., and D.L.B. contributed new reagents/analytic tools; Y.W. and B.B. analyzed data; and Y.W., E.M.Y.M., and B.B. wrote the paper.

Conflict of interest statement: B.B. and D.L.B. have financial interests in Tollbridge Therapeutics, LLC, which has licensed the patent for Diprovocim.

This article is a PNAS Direct Submission.

[1]To whom correspondence should be addressed. Email: bruce.beutler@utsouthwestern.edu.

This article contains supporting information online at www.pnas.org/lookup/suppl/doi:10.1073/pnas.1809232115/-/DCSupplemental.

Published online August 27, 2018.

Diprovocim elicits strong adjuvant activity in mice, successfully inhibiting tumor growth and prolonging survival when combined with a cancer antigen and immune checkpoint blockade in the B16-OVA melanoma model.

Results

Diprovocim Induces Cytokine Production in both Human and Mouse Cells. From a chemical library containing ~100,000 members, we identified a class of compounds with bilateral symmetry capable of activating TNF biosynthesis in phorbol 12-myristate 13-acetate (PMA)-differentiated human THP-1 myeloid cells. The initial members of the class emerged from an undisclosed compound sublibrary designed to promote cell surface receptor dimerization (18). Diprovocim (Fig. 1*A*) was developed from this class after extensive structure–activity relationship (SAR) studies. It induced dose-dependent TNF production by THP-1 cells (EC_{50} 110 pM) and human peripheral blood mononuclear cells (PBMC) (EC_{50} 875 pM) (Fig. 1 *B* and *C*) and by mouse peritoneal macrophages (EC_{50} 1.3 nM) and bone marrow-derived dendritic cells (BMDC) (EC_{50} 6.7 nM) (Fig. 1 *D* and *E*). In addition to TNF, Diprovocim induced IL-6 production by mouse BMDC (Fig. 1*F*). However, Diprovocim failed to stimulate type I IFN production by mouse peritoneal macrophages (*SI Appendix*, Fig. S1).

Diprovocim Targets TLR1/TLR2 and Activates Downstream MAPK and NF-κB Signaling Pathway. To determine the molecular target of Diprovocim, we analyzed its effects on peritoneal macrophages from wild-type C57BL/6J mice and C57BL/6J mice deficient in various TLR signaling components. Induction of TNF by Diprovocim was completely absent in TLR1- or TLR2-deficient macrophages but not in TLR-6 deficient macrophages (Fig. 2*A*). Diprovocim activity was also dramatically reduced in macrophages from MyD88-, TIRAP-, and IRAK4-deficient cells (Fig. 2*A*). These data suggest that Diprovocim targets the mouse TLR1/TLR2 heterodimer. TLR1 or TLR2 antibody significantly reduced the effect of Diprovocim on THP-1 cells, indicating that human TLR1/TLR2 is also a target of Diprovocim (Fig. 2*B*). Diprovocim induced phosphorylation of IKKα, IKKβ, p38, JNK, and ERK, as well as degradation of IκBα in THP-1 cells and mouse peritoneal macrophages, indicating that Diprovocim activates conventional TLR1/TLR2 signaling, including MAPK and canonical NF-κB signaling (Fig. 2 *C* and *D*).

Diprovocim Exhibits Adjuvant Activity in Vivo. Intramuscular immunization of wild-type mice with ovalbumin (OVA) plus either alum or Diprovocim induced similar levels of serum OVA-specific IgG, which were highly elevated compared with levels induced by immunization with OVA plus vehicle (Fig. 3 *A*–*C*). Whereas immunization with OVA + alum induced primarily the Th2-related Ig subclass IgG1, OVA + Diprovocim induced both IgG1 and the Th1-related IgG2b (Fig. 3 *B* and *C*).

DCs purified from draining lymph nodes and spleens 24 h after immunization of mice with OVA + Diprovocim activated OT-I CD8 T cells cocultured with them, as evidenced by CD69 up-regulation on the OT-I cells (Fig. 3*D*). In contrast, DCs from mice immunized with OVA + vehicle failed to induce CD69 expression on OT-I CD8 T cells (Fig. 3*D*). This finding suggests that Diprovocim activates antigen cross-presentation by DCs and cross-priming of CD8 T cells in vivo. To further investigate whether cross-priming stimulated by Diprovocim results in the development of killing ability by CD8+ T cells in vivo, a CTL killing assay was performed. Fluorescent labeled and OVA peptide

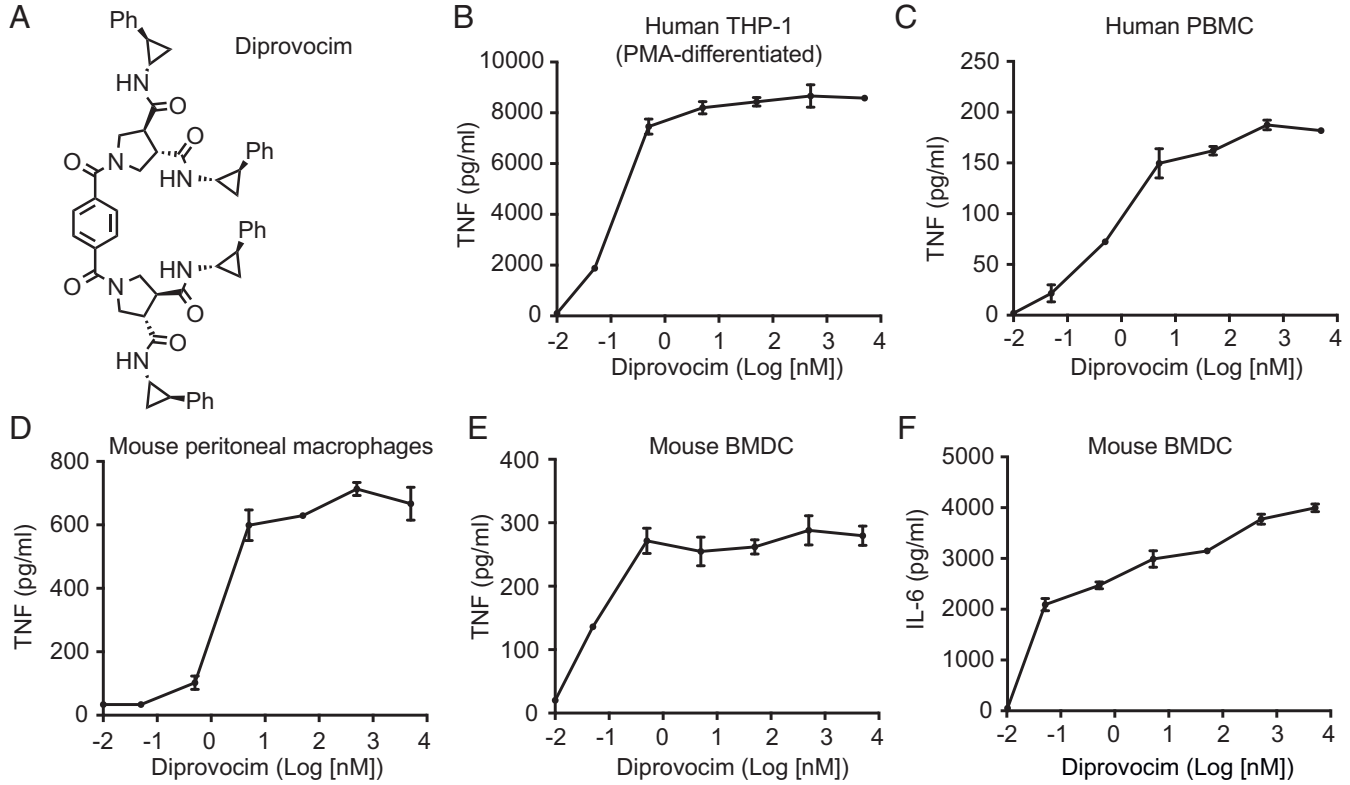

Fig. 1. Diprovocim induces cytokine secretion by mouse and human cells. (*A*) Chemical structure of Diprovocim. TNF in the supernatants of (*B*) human THP-1 cells, (*C*) human PBMC, (*D*) mouse peritoneal macrophages, or (*E*) mouse BMDC after treatment with Diprovocim for 4 h (*B*, *D*, and *E*) or 24 h (*C*). (*F*) IL-6 in the supernatants of mouse BMDC after treatment with Diprovocim for 4 h. In *B*–*F* the means of three independent samples are plotted. *P* values were determined by one-way ANOVA to compare the responses to different doses. In all experiments, $P < 0.0001$. Results in *B*–*F* are representative of two independent experiments.

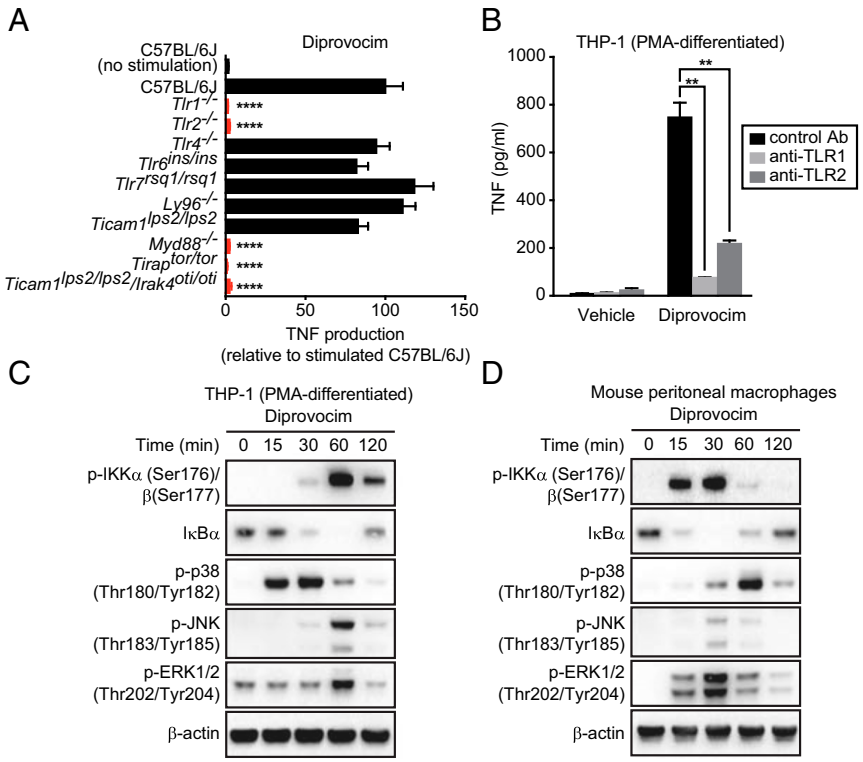

Fig. 2. Diprovocim activates mouse and human TLR1/TLR2. (*A*) TNF in the supernatants of mouse peritoneal macrophages of the indicated genotypes after treatment with Diprovocim (500 nM) for 4 h ($n = 3$ mice per genotype). Cytokine levels were normalized to those of stimulated C57BL/6J cells. *P* values were determined by Student's *t* test and represent the significance of differences between responses of stimulated C57BL/6J cells and stimulated cells of mutant genotypes; red bars indicate those with statistically significant differences. (*B*) TNF in the supernatants of human THP-1 cells pretreated with control antibody, anti-TLR1 (20 μg/mL), or anti-TLR2 (20 μg/mL) for 1 h, followed by treatment with vehicle or Diprovocim (250 pM) for another 4 h. *P* values were determined by Student's *t* test. Immunoblot analysis of lysates of (*C*) human THP-1 cells and (*D*) mouse peritoneal macrophages treated with Diprovocim (5 nM in THP-1 and 500 nM in mouse peritoneal macrophages) for the indicated times. In *A* and *B* the means of three independent samples are plotted. All results are representative of two independent experiments.

(aa 257–263)-pulsed target cells were injected i.v. into mice immunized with OVA + Diprovocim, and the number of live target cells was measured by flow cytometry 2 d later. About 70% of target cells had been eliminated in mice immunized with OVA + Diprovocim, compared with ∼10% in mice immunized with OVA + vehicle (Fig. 3*E*). These data demonstrate that Diprovocim exhibits adjuvant activity in antigen-specific antibody production and CTL killing, which was abrogated in TLR1- and/or TLR2-deficient mice (Fig. 3 *A*–*C*, *F*, and *G*).

Complete Inhibition of B16 Tumor Growth by Combined Checkpoint Blockade and Anticancer Vaccine Adjuvanted with Diprovocim. We tested the adjuvant activity of Diprovocim in preventive immunization of wild-type mice against B16 melanoma expressing OVA (B16-OVA) (Fig. 4*A*). Mice were injected i.m. distal to the tumor cell injection site with OVA with or without Diprovocim on the same day but before inoculation with B16-OVA cells. Tumor growth rates and survival times were similar for mice immunized with vehicle alone, Diprovocim alone, or OVA alone (Fig. 4 *B* and *C*). Relative to OVA alone, immunization with Diprovocim + OVA modestly but significantly slowed tumor growth rate but failed to prolong survival; a similar effect was observed with OVA immunization combined with anti–PD-L1 treatment (Fig. 4 *B* and *C*). Strikingly, although without effect by itself (*SI Appendix*, Fig. S2), when anti–PD-L1 treatment was added to Diprovocim + OVA immunization, there was complete inhibition of tumor growth and 100% survival through 8 wk of observation (Fig. 4 *B* and *C*). This dramatic antitumor effect was dependent on OVA immunization because Diprovocim alone combined with anti–PD-L1 treatment had no effect on tumor growth or mouse survival (Fig. 4 *D* and *E*); this finding is consistent with poor immunogenicity of B16 melanoma (19–21).

To determine whether surviving mice were endowed with specific and long-term memory directed against the cancer antigen, we rechallenged the 5-wk survivors from Fig. 4*C* with B16-OVA cells and B16 cells lacking OVA (B16). In the absence of any further therapy, we observed complete failure of B16-OVA tumor growth, whereas B16 tumors grew rapidly (Fig. 4*F*). Both B16 and B16-OVA tumor cells grew at similar rates in naïve C57BL/6J mice (Fig. 4*F*). Taken together, these data indicate that when used as an adjuvant in a cancer vaccine, Diprovocim promotes antigen-specific antitumor immunity, which is greatly enhanced when combined with T cell checkpoint blockade in mice. Immunization with Diprovocim as an adjuvant produces antigen-specific memory responses that protect the host from relapse of tumor growth.

We tested the antitumor effect of Diprovocim in therapeutic immunization of mice with already established B16-OVA tumors. C57BL/6J mice were immunized with OVA with or without Diprovocim on the day of or 3 d after tumor inoculation and received a booster immunization 7 d later (Fig. 4*A*). In some mice, alum was substituted for Diprovocim to permit direct comparison between these two adjuvants. For all conditions, anti–PD-L1 treatment was initiated on day 3 after tumor inoculation and repeated every 3 d thereafter for 12 d. Mice immunized with OVA alone on the day of tumor inoculation survived an average of 24 d, and 100% of mice (8/8) died by 38 d after tumor inoculation. As expected, Diprovocim + OVA administered on the day of tumor

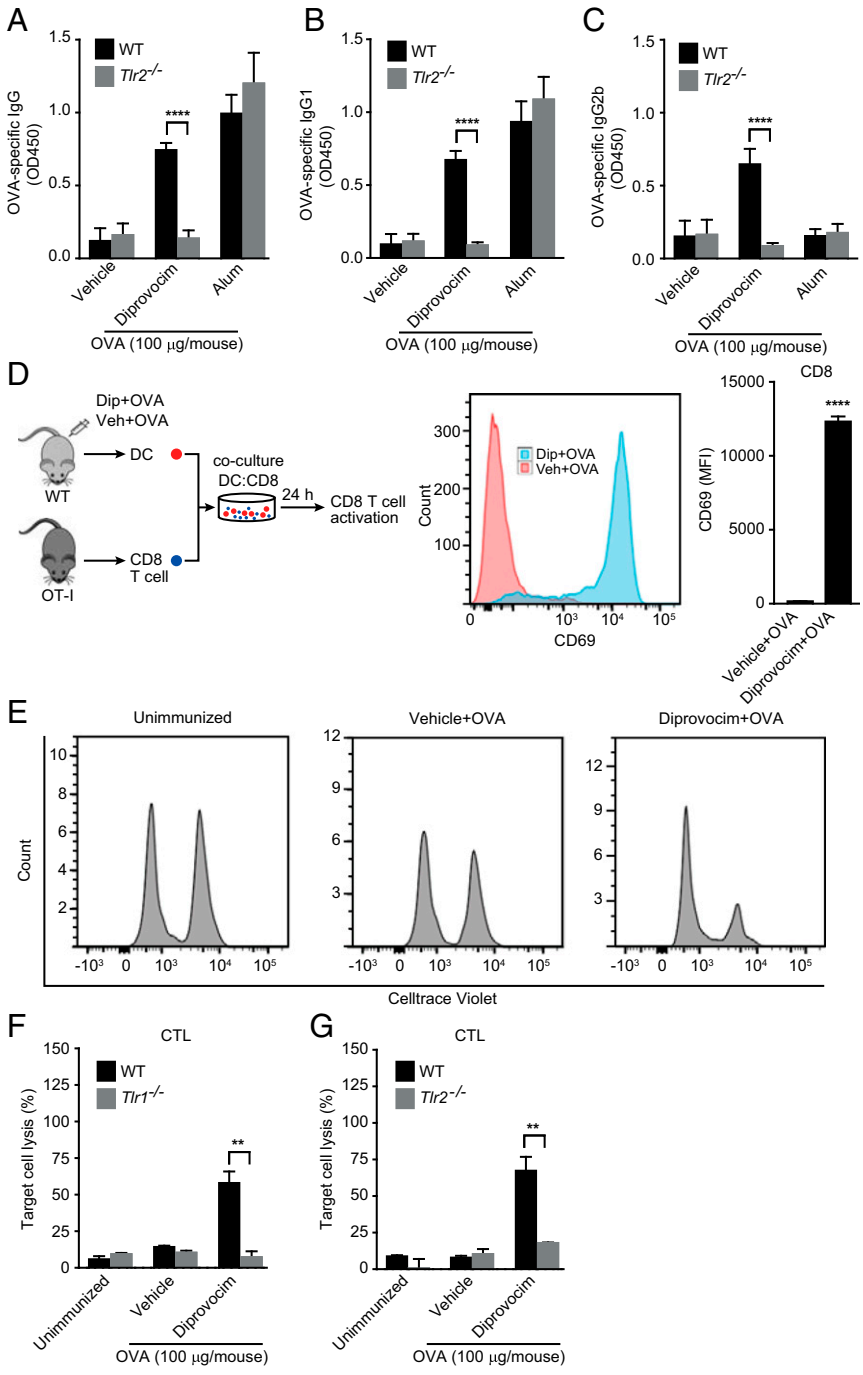

Fig. 3. Diprovocim enhances antigen-specific antibody and CTL responses. (*A–C*) WT or *Tlr2*$^{-/-}$ C57BL/6J mice (four mice per group) were immunized i.m. with 100 μg OVA mixed with vehicle, Diprovocim (10 mg/kg), or alum (2 mg/kg). After 14 d, serum titers of OVA-specific IgG (*A*), OVA-specific IgG1 (*B*), and OVA-specific IgG2b (*C*) were measured by ELISA. (*D*) Experimental setup (*Left*) for detection (*Center*) and quantification (*Right*) of CD69 expression on OT-I CD8 T cells by flow cytometry after 24 h coculture with DC collected from mice 24 h after they were immunized i.m. with OVA mixed with vehicle or Diprovocim (four mice per group). (*E* and *F*) Mice were unimmunized or immunized i.m. with 100 μg OVA mixed with vehicle or Diprovocim (10 mg/kg) (four mice per group). Seven days after immunization, mice were injected i.v. with Celltrace Violet-labeled mouse splenocytes that were unpulsed (control cells) or pulsed with OVA peptide (aa 257–263) (target cells). Two days later, blood was collected to measure remaining live dye-labeled cells. (*E*) Representative flow cytometry plots show count of remaining target cells (right peak) and control cells (left peak) in wild-type mice. (*F* and *G*) Quantitative comparison of the percentage of target cells killed in WT, *Tlr1*$^{-/-}$, or *Tlr2*$^{-/-}$ mice. *P* values were determined by Student's *t* test. All results are representative of two independent experiments.

inoculation completely inhibited tumor growth, permitting 100% of mice (8/8) to survive through 54 d of observation (Fig. 4 *G* and *H*). When alum was used instead of Diprovocim in the same experiment, tumor growth was partially inhibited, and the average survival time was 37 d, with 25% of mice (2/8) surviving past 54 d (Fig. 4 *G* and *H*). When immunization was delayed until 3 d after tumor inoculation, Diprovocim + OVA still significantly inhibited tumor growth and prolonged average survival compared with OVA alone (41 d vs. 22 d) (Fig. 4 *I* and *J*). In contrast, alum + OVA inhibited tumor growth but only slightly increased average

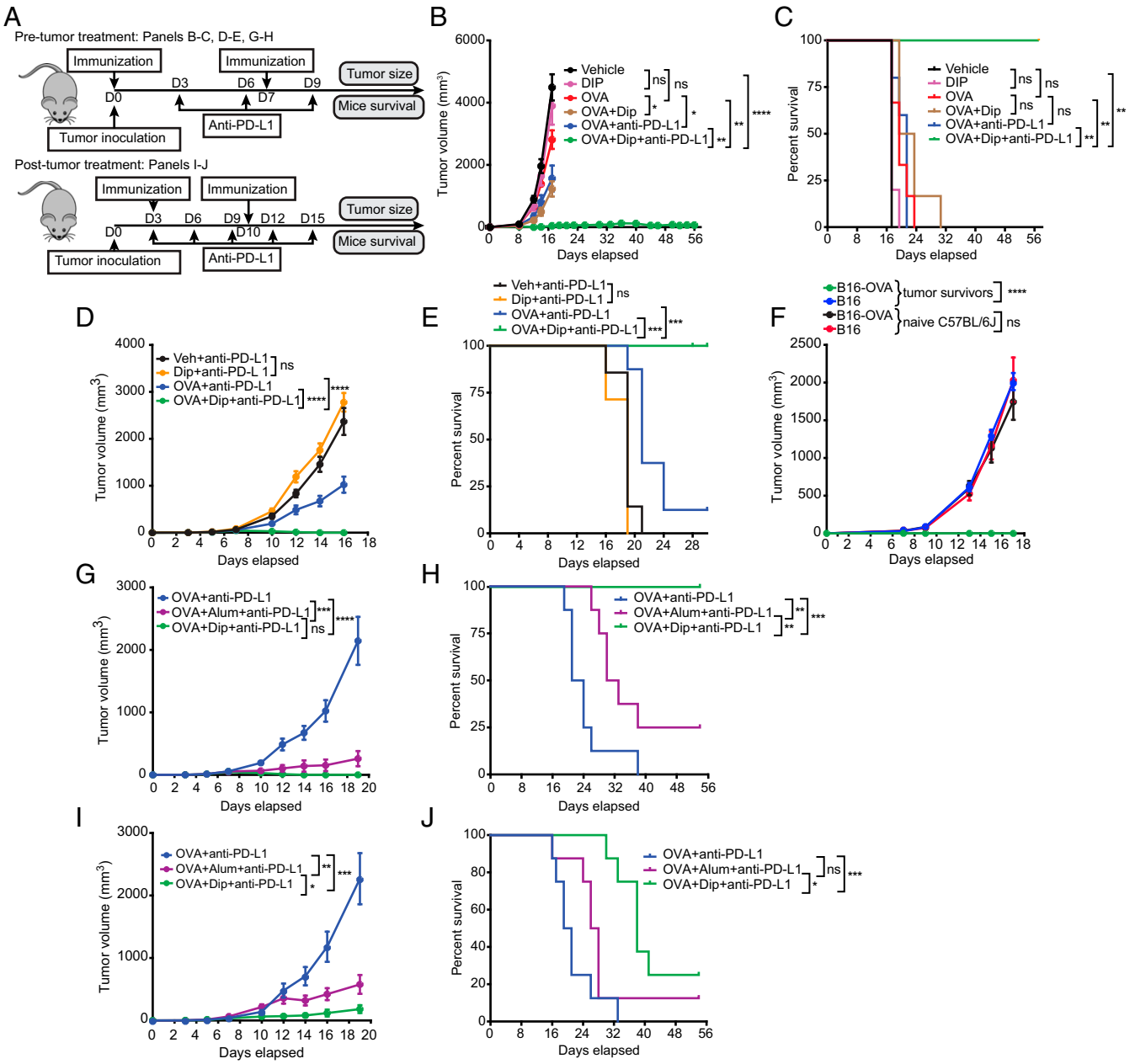

Fig. 4. Inhibition of B16-OVA tumor growth by pretumor or posttumor treatment with Diprovocim-adjuvanted tumor vaccination and checkpoint blockade. (*A*) Schematic of pretumor and posttumor treatment protocols. C57BL/6J mice ($n = 8$ mice per treatment) were injected s.c. with 2×10^5 B16-OVA melanoma cells on day 0. For pretumor treatment, mice were immunized i.m. with OVA (100 μg) mixed with vehicle or Diprovocim (10 mg/kg) or alum (2 mg/kg) on the same day before tumor injection. Mice received a booster immunization 7 d later. Anti–PD-L1 (200 μg) was administered on day 3, 6, and 9 after tumor inoculation by i.p. injection. For posttumor treatment, initial immunization was on day 3 after tumor inoculation, with a booster 7 d later. Anti–PD-L1 (200 μg) was administered on day 3, 6, 9, 12, and 15 after tumor inoculation by i.p. injection. (*B–E*) Pretumor treatment. Tumor volume (*B* and *D*) and percent mouse survival (survivors/total mice) (*C* and *E*). (*F*) Naïve mice (black and red, $n = 8$) or day 35 tumor-free survivors (blue and green, $n = 8$) from *C* were challenged with 2×10^5 cells each of B16-OVA (green and black) and B16F10 tumor cells (blue and red) by s.c. injection, and tumor volume was monitored. (*G–J*) Comparison of pretumor (*G* and *H*) vs. posttumor treatment (*I* and *J*). Tumor volume (*G* and *I*) and percent mouse survival (survivors/total mice) (*H* and *J*). *P* values for tumor volume analysis apply to the final time point as indicated in graphs and were calculated by Student's *t* test. *P* values for survival analysis were calculated by Kaplan–Meier analysis. All results are representative of two independent experiments.

survival time (30 d); the survival curve for alum + OVA was not significantly different from the curve for OVA alone ($P = 0.082$) (Fig. 4 *I* and *J*). In pretumor and posttumor treatment, the effect of Diprovocim on tumor growth, survival rate, and survival time was superior to that of alum.

Diprovocim Enhances Antitumor CTL Responses. To investigate the cellular mechanism by which combined anti–PD-L1 treatment and Diprovocim-adjuvanted immunization eliminates tumors, we analyzed the tumor-infiltrating leukocytes (TILs) of mice immunized with Diprovocim + OVA or alum + OVA 3 d after tumor inoculation (Fig. 5*A*). Tumors were collected 14 d after inoculation, and single-cell suspensions were antibody stained and analyzed by flow cytometry to detect total leukocytes, CD4 and CD8 T cells, NK cells, DCs, and macrophages. The leukocytes were also stained with antibody to the H-2K^b MHC-class

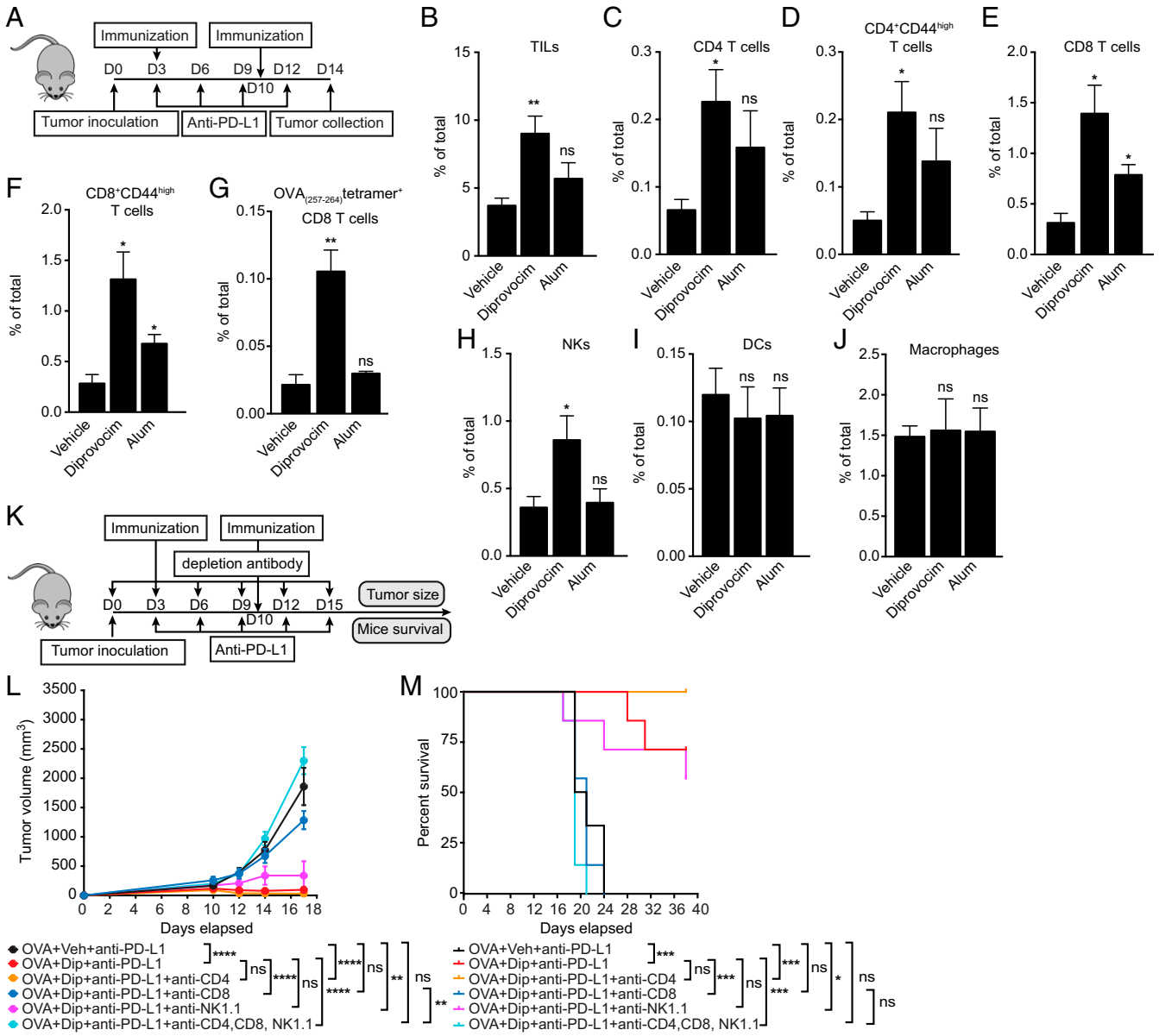

Fig. 5. Diprovocim enhances TILs and antitumor CTL responses. (*A*) Schematic of treatment protocol for *B*–*J*. C57BL/6J mice ($n = 6$ mice per treatment) were injected s.c. with 2×10^5 B16-OVA melanoma cells on day 0 and 3 d later, immunized i.m. with OVA (100 μg) mixed with vehicle or Diprovocim (10 mg/kg) or alum (2 mg/kg). Mice received a booster immunization on day 10 after tumor inoculation. Anti–PD-L1 (200 μg) was administered on day 3, 6, 9, and 12 after tumor inoculation by i.p. injection. Tumors were harvested on day 14 to isolate and analyze TILs. (*B*–*J*) The frequency of each cell type out of total tumor cells is shown. (*B*) TILs ($CD45^+$). (*C*) CD4 T cells ($CD4^+CD3^+CD45^+$). (*D*) Activated CD4 T cells ($CD44^{high}CD4^+CD3^+CD45^+$). (*E*) CD8 T cells ($CD8^+CD3^+CD45^+$). (*F*) Activated CD8 T cells ($CD44^{high}CD8^+CD3^+CD45^+$). (*G*) OVA-specific CD8 T cells bearing a T-cell receptor specific for $OVA_{(257-264)}$-H2Kb tetramer. (*H*) NK cells ($NK1.1^+CD3^-CD45^+$). (*I*) DCs ($CD11c^+CD3^-CD45^+$). (*J*) Macrophages ($F4/80^+CD11b^+CD45^+$). (*K*) Schematic of treatment protocol for *L* and *M*. C57BL/6J mice ($n =$ 8 mice per treatment) were injected s.c. with 2×10^5 B16-OVA melanoma cells on day 0 and 3 d later, immunized i.m. with OVA (100 μg) mixed with vehicle or Diprovocim (10 mg/kg). Mice received a booster immunization on day 10 after tumor inoculation. Anti–PD-L1 (200 μg) was administered on day 3, 6, 9, 12, and 15 after tumor inoculation by i.p. injection. On day 0, 3, 6, 9, 12, and 15, anti-CD4 (300 μg), anti-CD8 (300 μg), anti-NK1.1 (300 μg), or a mixture of these three antibodies was administered to C57BL/6J mice by i.p. injection. (*L*) Tumor volume and (*M*) percent mouse survival (survivors/total mice). *P* values for tumor volume analysis apply to the final time point as indicated in graphs and were calculated by Student's *t* test. *P* values for survival analysis were calculated by Kaplan–Meier analysis. All results are representative of two independent experiments.

I tetramer bound to the OVA peptide (aa 257–264), as well as antibody against CD8 to identify tumor-specific CD8 T cells. OVA immunizations containing Diprovocim significantly increased the frequency of leukocytes in tumors compared with vehicle + OVA (Fig. 5*B*). Further analysis of these TILs revealed that Diprovocim increased the frequencies of CD4 and CD8 T cells including activated CD4 and CD8 T cells ($CD44^{high}$) and OVA-specific CD8 T cells, as well as the frequency of NK cells (Fig. 5 *C*–*H*). Alum + OVA immunization showed a trend toward increasing TILs (Fig. 5*B*), which reached statistical significance for total and $CD44^{high}$ CD8 T cells (Fig. 5 *E* and *F*); however, the magnitude of the increase was reduced compared with that induced by Diprovocim + OVA. OVA-specific CD8 T cells were not increased by alum + OVA immunization (Fig. 5*G*) on day 14 after tumor inoculation; neither were total and $CD44^{high}$ CD4 T cells (Fig. 5 *C* and *D*), nor NK cells compared

with vehicle + OVA (Fig. 5*H*). The frequencies of intratumor DCs and macrophages were similar for mice immunized with vehicle + OVA, Diprovocim + OVA, and alum + OVA (Fig. 5 *I* and *J*). Overall, these data indicate that the intratumor frequencies of CD4 and CD8 T cells, activated CD4 and CD8 T cells, OVA-specific CD8 T cells, and NK cells, but not DCs or macrophages, correlated with the antitumor effects of Diprovocim and alum in immunized mice.

To determine the immune cell population(s) necessary for the antitumor effect of Diprovocim + OVA plus anti–PD-L1, we depleted mice of CD8 T cells, CD4 T cells, NK cells, or all three cell populations using cell type-specific antibodies. The depletion antibodies were administered i.p. on the day of B16-OVA tumor inoculation (day 0) and every 3 d thereafter for 15 d (Fig. 5*K*). The effect of Diprovocim + OVA on both tumor growth and mouse survival was abrogated when mice were depleted of CD8 T cells or all three cell types together (CD4 T, CD8 T, and NK cells) (Fig. 5 *L* and *M*). In contrast, depletion of CD4 T cells or NK cells had little effect on the antitumor activity of Diprorocim + OVA (Fig. 5 *L* and *M*). We noted a slight, statistically significant difference between the effects of CD8 T cell depletion vs. CD4 + CD8 + NK cell depletion on tumor growth in mice treated with Diprovocim + OVA plus anti–PD-L1, in which tumor growth was greater in mice depleted of all three cell types. However, this difference did not translate to a difference in either survival rate or time. This finding suggests a minor role of either CD4 T cells, NK cells, or both, in mediating the antitumor effects of Diprovocim + OVA plus anti–PD-L1. These data demonstrate that CD8 T cells are necessary for tumor eradication by therapeutic Diprovocim + OVA immunization and checkpoint inhibition in mice.

Discussion

It is believed that cancer vaccines targeted to tumor neoantigens can boost the success of immune checkpoint inhibition for cancer treatment by increasing the number and activation of tumor-specific CTLs capable of responding to checkpoint inhibitors. However, the type and magnitude of the T cell response to immunization depends critically on the vaccine adjuvant; currently, only few adjuvants are approved for use in humans. Here we describe the actions of a potent adjuvant, Diprovocim, that engages and activates human and mouse TLR1/TLR2 heterodimers. Diprovocim bears no structural similarity to other reported synthetic chemical ligands, nor to the natural ligands that activate TLR1/TLR2 (22–26). Diprovocim is more potent and efficacious in activating human TLR1/TLR2 than Pam_3CSK_4 (*SI Appendix*, Fig. S3), a well-known ligand. In mice, Diprovocim induces strong TLR1- and TLR2-dependent humoral and CTL responses to a coadministered antigen. When combined with checkpoint inhibition, Diprovocim-adjuvanted immunization causes antigen-specific eradication of a rapidly fatal tumor and induces memory responses capable of preventing tumor regrowth. Cure of the tumor is observed despite the fact that checkpoint inhibition alone is insufficient to prevent a fatal outcome (*SI Appendix*, Fig. S2), supporting the premise of this combination immunotherapy.

Our data support the following key mechanistic events mediating the antitumor effect of Diprovocim-adjuvanted immunization plus checkpoint inhibition (Fig. 6). Diprovocim binds to TLR1/TLR2 on APCs, activating them to produce proinflammatory cytokines and take up the administered tumor-specific antigens for processing and presentation via MHC I and MHC II. Antigen presentation, costimulatory molecule expression, and cytokine secretion by APCs induce proliferation and activation of antigen-specific CD4 T cells and CD8 T cells, which develop cytolytic activity toward tumor cells. NK cells are also activated by proinflammatory cytokines and infiltrate the tumor site. The addition of anti–PD-L1 inhibits the major immunosuppressive

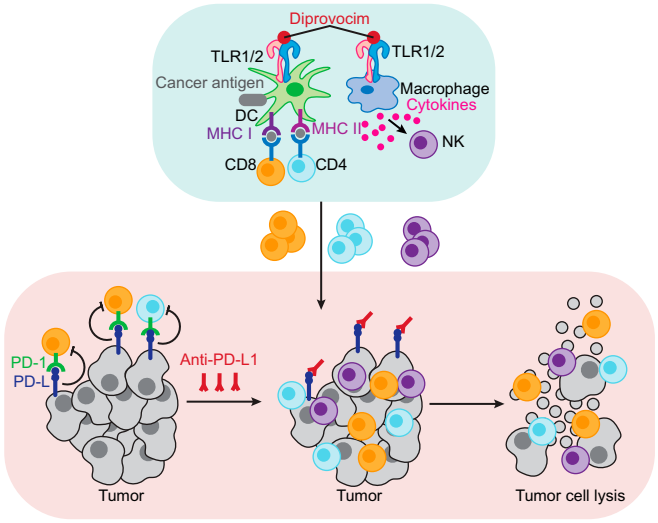

Fig. 6. Model of key cellular events mediating the antitumor effect of Diprovocim-adjuvant immunization plus checkpoint inhibition. See text for details.

mechanism active in the tumor microenvironment, permitting uninhibited T cell activation and proliferation in response to TCR/CD28 ligation (27–29), further promoting tumor cell lysis mediated by CD8 T cells.

Numerous reports document both protumorigenic and antitumorigenic effects of TLR2 signaling, which may depend on the cell type or type of cancer under study. For example, TLR2 signaling supports tumor growth through induction of immune suppressive cytokines such as IL-10 and activation of myeloid-derived suppressor cells and tumor-associated macrophages (30–32). In contrast, TLR2 signaling also promotes tumor regression by stimulating DC activation and cross-presentation (33) and down-regulating Treg function (34–36). We found that for Diprovocim, the overall outcome of systemic TLR2 activation, in the context of OVA immunization combined with immune checkpoint inhibition, was tumor cell lysis and tumor growth inhibition mediated by tumor-infiltrating antigen-specific CD8 T cells.

The therapeutic index of an adjuvant presumably depends upon the efficiency of conjoint targeting of antigen to an APC and activation of that APC. The mode of interaction between Diprovocim and TLR2 has been studied by X-ray crystallography, and its contacts with this subunit of the receptor will be reported elsewhere. The structure of the Diprovocim–TLR1/TLR2 complex points to opportunities for Diprovocim modification to incorporate immunogenic peptides, which might allow optimization of the therapeutic index by assuring that all active Diprovocim molecules are accompanied by antigen. Diprovocim is easy to synthesize and can be rapidly adapted to incorporate tumor-associated antigens and neoantigens. These features make it an attractive candidate for clinical development.

Materials and Methods

Synthesis of Diprovocim. The protocol for synthesis of Diprovocim is provided in *SI Appendix*.

Mice. C57BL/6J, $Tlr2^{-/-}$, $Myd88^{-/-}$, and OT-I mice were purchased from The Jackson Laboratory. $Ly96^{-/-}$ ($MD\text{-}2^{-/-}$) mice were from Riken BioResource Research Center. $Tlr4^{lps3/lps3}$, $Tlr6^{int/int}$, $Tlr7^{rsq1/rsq1}$, $Tirap^{tor/tor}$, $Ticam1^{Lps2/Lps2}$, and $Ticam1^{Lps2/Lps2}$/$Irak4^{otiose/otiose}$ mice were generated on a pure C57BL/6J background by ENU mutagenesis and are described at mutagenetix.utsouthwestern.edu.

$Tlr1^{-/-}$ mice were created by CRISPR/Cas 9 gene targeting. Female C57BL/6J mice were superovulated by injection of 6.5 U pregnant mare serum gonadotropin (PMSG; Millipore), followed by injection of 6.5 U human CG (hCG; Sigma–Aldrich) 48 h later. The superovulated mice were subsequently mated overnight with C57BL/6J male mice. The following day, fertilized eggs were

collected from the oviducts, and in vitro-transcribed Cas9 mRNA (50 ng/μL) and Tlr1 small base-pairing guide RNA (50 ng/μL; 5′-CAAACCGATCGTAGTGCTGA-3′) were injected into the cytoplasm or pronucleus of the embryos. The injected embryos were cultured in M16 medium (Sigma–Aldrich) at 37 °C in 5% CO_2. For the production of mutant mice, two-cell stage embryos were transferred into the ampulla of the oviduct (10–20 embryos per oviduct) of pseudopregnant Hsd:ICR (CD-1) female mice (Harlan Laboratories).

All experimental procedures using mice were approved by the Institutional Animal Care and Use Committee of the University of Texas Southwestern Medical Center and were conducted in accordance with institutionally approved protocols and guidelines for animal care and use. All of the mice were maintained at the University of Texas Southwestern Medical Center in accordance with institutionally approved protocols.

Isolation of Peritoneal Macrophages, BMDC, Human PBMC, and Cell Culture. Thioglycollate-elicited macrophages were recovered 4 d after i.p. injection of 2 mL BBL thioglycollate medium, brewer modified (4% wt/vol; BD Biosciences) by peritoneal lavage with 5 mL PBS. The peritoneal macrophages were cultured in DMEM cell culture medium [DMEM containing 10% vol/vol FBS (Gemini Bio Products), 1% vol/vol penicillin and streptomycin (Life Technologies)] at 37 °C and 95% air/5% CO_2. For murine BMDCs, bone marrow cells were cultured in Petri dishes in 10 mL DMEM cell culture medium containing 10 ng/mL of murine GM-CSF (R&D Systems). On day 3 of culture, this was replaced with fresh GM-CSF medium. Loosely adherent cells were transferred to a fresh Petri dish and cultured for an additional 4 d. Human PBMC were purchased from Stemcell Technologies. THP-1 (American Type Culture Collection) cells were differentiated by treatment with 100 nM PMA (Sigma) in Roswell Park Memorial Institute (RPMI) cell culture medium [RPMI containing 10% vol/vol FBS (Gemini Bio Products), 1% penicillin and streptomycin (Life Technologies)] for 24 h. After that, cells were washed with PBS and cultured in fresh RPMI cell culture medium for 24 h before use in experiments.

Measurement of Cytokine Production. Cells were seeded onto 96-well plates at 1×10^5 cells per well and stimulated with Diprovocim [dissolved in DMSO, and final DMSO concentrations (≤0.2%) were kept constant in all experiments] for 4 h. Mouse TNF, IL-6, or IFN-β or human TNF in the supernatants were measured by ELISA kits according to the manufacturer's instructions (eBioscience and PBL Assay Science). Pretreatment with 20 μg/mL anti-TLR1, anti-TLR2, or isotype control antibody (eBioscience) was for 1 h. Unless otherwise indicated, mouse cells were from wild-type C57BL/6J mice.

Western Blotting. Mouse peritoneal macrophages or human THP-1 cells (1×10^6 per well) were stimulated in 12-well plates with Diprovocim at 500 nM for mouse cells or 5 nM for human cells for the indicated times and lysed directly in sample buffer (Sigma). Cell lysates were separated by SDS/PAGE and transferred to nitrocellulose membranes. Membranes were probed with the following antibodies: phospho-IKKα (Ser176)/IKKβ (Ser177), IκBα, phospho-p38 (Thr180/Tyr182), phospho-JNK (Thr183/Tyr185), phospho-ERK1/2 (Thr202/Tyr204) (Cell Signaling Technology), and β-Actin (Sigma).

Immunization and Measurement of Antibody Response. EndoFit ovalbumin (OVA) with ≥98% purity minimum (SDS/PAGE) and endotoxin levels <1 EU/mg was purchased from Invivogen. Mice (four mice per group) were immunized i.m. with 100 μg OVA mixed with vehicle (DMSO:Tween 80:saline = 1:1:8), with 10 mg/kg Diprovocim, or with 2 mg/kg Alum (Alhydrogel adjuvant 2%; Invivogen). After 14 d, serum titers of OVA-specific IgG, IgG1, or IgG2b (SouthernBiotech) were measured by ELISA.

In Vivo CTL Killing Assay. C57BL/6J male mice were injected i.m. with 100 μg OVA plus 10 mg/kg Diprovocim ($n = 4$ mice per group). One week later, naive C57BL/6J mice were killed, and splenocytes were collected. Half of the splenocytes were left unpulsed, and half were pulsed with OVA257–263 peptides for 2 h in complete medium (RPMI containing 10% vol/vol FBS, 1% penicillin and streptomycin) at 37 °C. The unpulsed and peptide-pulsed cells were labeled with 0.5 μM (low) or 5 μM (high) CellTrace Violet (Invitrogen), respectively, in serum-free medium for 20 min. Equal numbers (2×10^6) of CellTrace Violet^{high} (OVA pulsed) and CellTrace Violet^{low} (unpulsed) cells were mixed together and injected i.v. into the immunized mice. After 48 h, blood from treated mice was collected and subjected to flow cytometry analysis. The numbers of remaining live CellTrace Violet^{high} and CellTrace Violet^{low} cells were determined and used to calculate the percentage of OVA peptide-pulsed target cells killed. Specific killing was defined as the ratio = CellTrace Violet^{low} cells/CellTrace Violet^{high} cells. The percentage of target cell lysis = (1 − unimmunized ratio/immunized ratio) × 100.

Tumor Inoculation, Immunization, and Tumor Measurement. B16-OVA cells (B16F10 melanoma cells stably expressing chicken ovalbumin) were grown in DMEM containing 10% vol/vol FBS. A total of 2×10^5 B16-OVA cells in 100 μL PBS were injected s.c. into the right flank of 8- to 12-wk-old male C57BL/6J mice to establish tumors ($n = 8$ mice per group). For pretreatment, 10 mg/kg Diprovocim or 2 mg/kg alum with or without OVA (100 μg) was injected i.m. into mice on the same day as tumor inoculation (day 0). Mice received a booster shot 7 d after the first immunization. On day 3, 6, and 9, some groups were injected i.p. with 200 μg checkpoint inhibitor (anti–mPD-L1; BioXcell) in 100 μL saline. For posttreatment, 10 mg/kg Diprovocim or 2 mg/kg Alum with OVA (100 μg) was injected i.m. into mice on day 3 after tumor inoculation. Mice received a booster shot 7 d after the first immunization. On day 3, 6, 9, 12, and 15 after tumor inoculation, mice were also injected i.p. with 200 μg anti–mPD-L1 in 100 μL saline. For depletion of CD4 T cells, CD8 T cells, and/or NK cells, 300 μg anti-mCD4 (BioXcell), 300 μg anti-mCD8 (BioXcell), 300 μg anti-mNK1.1 (BioXcell), or the three antibodies together in 200 μL saline were injected i.p. into mice on day 0, 3, 6, 9, 12, and 15 after tumor inoculation. On day 3 after tumor inoculation, 10 mg/kg Diprovocim with OVA (100 μg) or vehicle was injected i.m. into mice. Mice received a booster shot 7 d after the first immunization. On day 3, 6, 9, 12, and 15 after tumor inoculation, mice were also injected i.p. with 200 μg anti–mPD-L1 in 100 μL saline. Tumors were measured with a digital caliper (Fisher), and the tumor sizes were calculated using the following formula: volume = $0.5 \times \text{length} \times \text{width}^2$. Mice were killed when the tumor length or width reached 2 cm.

Tumor-Infiltrating Leukocyte Separation and Staining. A total of 2×10^5 B16-OVA cells in 100 μL PBS were injected s.c. into the flank of each mouse to establish tumors ($n = 6$ mice per treatment). On day 3 after tumor inoculation, 10 mg/kg Diprovocim or 2 mg/kg alum with OVA (100 μg) was injected i.m. into mice. Mice received a booster shot 7 d after the first immunization. On day 3, 6, 9, and 12 after tumor inoculation, mice were also injected i.p. with 200 μg anti–mPD-L1. On day 14 after tumor inoculation, tumors were harvested, minced, and filtered through a 40-μm strainer to obtain single-cell suspensions. Red blood cells were lysed with RBC lysis buffer (Sigma). After pelleting, cells were stained with a mixture of antibodies for 45 min, including anti-mouse CD45.2-PE or CD45.2-APC (BioLegend), anti-mouse CD3-FITC (BD Biosciences), anti-mouse CD4-BV786 (BD Biosciences), anti-mouse CD8-BV510 (BioLegend), anti-mouse CD44-PE-CF594 (BioLegend), APC-conjugated H-2Kb/OVA (SIINFEKL) tetramer (Baylor College of Medicine), anti-mouse F4/80-PE (Tonbo Bioscience), anti-mouse CD11b-BV605 (BioLegend), anti–CD11c-BV711 (BD Biosciences), and anti–NK1.1-BV650 (BD Biosciences). Then, the cells were washed twice with PBS. Stained cells were analyzed with an LSR II flow cytometer (BD Biosciences), and the flow cytometry data were analyzed using FlowJo software.

Measurement of Cross-Priming of CD8 T Cells. C57BL/6J male mice were injected i.m. with 100 μg OVA mixed with vehicle or with 10 mg/kg Diprovocim ($n = 4$ mice per treatment). Twenty-four hours later, DCs from draining lymph nodes and spleen were purified by Mouse Pan Dendritic Cell Isolation Kit (Miltenyi Biotech). CD8 T cells from OT-I transgenic mice were purified by Mouse CD8+ T Cell Isolation Kit (Miltenyi Biotech). Then, 3×10^5 DCs were cocultured with 3×10^5 OT-I CD8 T cells in RPMI medium containing 10% vol/vol FBS and 1% vol/vol penicillin and streptomycin for 24 h. Then, cells were collected and stained with anti-mouse CD3-FITC, anti-mouse CD8-BV510, and anti-mouse CD69-PE-CF594 (BioLegend) for 45 min. Then, the cells were washed twice with PBS. Stained cells were analyzed with an LSRII instrument, and the flow cytometry data were analyzed using FlowJo software.

Statistical Analyses. Data represent means ± SEM in all graphs depicting error bars. The statistical significance of differences between experimental groups was determined using GraphPad Prism 7 and the indicated statistical tests. For comparisons of differences between two unpaired experimental groups, an unpaired Student's *t* test was used, and two-tailed *P* values are reported. *P* values are indicated by $^*P \le 0.05$, $^{**}P \le 0.01$, $^{***}P \le 0.001$, and $^{****}P \le 0.0001$. $P \le 0.05$ was considered statistically significant.

ACKNOWLEDGMENTS. We thank Diantha La Vine for expert assistance with figure preparation. This work was supported by NIH Grants AI125581 (to B.B.), CA042056 (to D.L.B.), and AI082657 (to D.L.B.), and by the Lyda Hill foundation (B.B.).

1. Hou B, Reizis B, DeFranco AL (2008) Toll-like receptors activate innate and adaptive immunity by using dendritic cell-intrinsic and -extrinsic mechanisms. *Immunity* 29: 272–282.
2. MacLeod H, Wetzler LM (2007) T cell activation by TLRs: A role for TLRs in the adaptive immune response. *Sci STKE* 2007:pe48.
3. Coffman RL, Sher A, Seder RA (2010) Vaccine adjuvants: Putting innate immunity to work. *Immunity* 33:492–503.
4. Haanen JBAG (2017) Converting cold into hot tumors by combining immunotherapies. *Cell* 170:1055–1056.
5. Sharma P, Hu-Lieskovan S, Wargo JA, Ribas A (2017) Primary, adaptive, and acquired resistance to cancer immunotherapy. *Cell* 168:707–723.
6. Wang H, et al. (2017) cGAS is essential for the antitumor effect of immune checkpoint blockade. *Proc Natl Acad Sci USA* 114:1637–1642.
7. Zou W, Wolchok JD, Chen L (2016) PD-L1 (B7-H1) and PD-1 pathway blockade for cancer therapy: Mechanisms, response biomarkers, and combinations. *Sci Transl Med* 8:328rv4.
8. Topalian SL, Drake CG, Pardoll DM (2015) Immune checkpoint blockade: A common denominator approach to cancer therapy. *Cancer Cell* 27:450–461.
9. Takeda Y, et al. (2017) A TLR3-specific adjuvant relieves innate resistance to PD-L1 blockade without cytokine toxicity in tumor vaccine immunotherapy. *Cell Rep* 19: 1874–1887.
10. Shah RR, Hassett KJ, Brito LA (2017) Overview of vaccine adjuvants: Introduction, history, and current status. *Methods Mol Biol* 1494:1–13.
11. Reed SG, Orr MT, Fox CB (2013) Key roles of adjuvants in modern vaccines. *Nat Med* 19:1597–1608.
12. Kawai T, Akira S (2010) The role of pattern-recognition receptors in innate immunity: Update on Toll-like receptors. *Nat Immunol* 11:373–384.
13. Kawasaki T, Kawai T (2014) Toll-like receptor signaling pathways. *Front Immunol* 5: 461.
14. Beutler BA (2009) TLRs and innate immunity. *Blood* 113:1399–1407.
15. Lim KH, Staudt LM (2013) Toll-like receptor signaling. *Cold Spring Harb Perspect Biol* 5:a011247.
16. Wang S, et al. (2016) Intratumoral injection of a CpG oligonucleotide reverts resistance to PD-1 blockade by expanding multifunctional CD8+ T cells. *Proc Natl Acad Sci USA* 113:E7240–E7249.
17. Dowling JK, Mansell A (2016) Toll-like receptors: The Swiss Army knife of immunity and vaccine development. *Clin Transl Immunology* 5:e85.
18. Goldberg J, et al. (2002) Erythropoietin mimetics derived from solution phase combinatorial libraries. *J Am Chem Soc* 124:544–555.
19. Ueha S, et al. (2015) Robust antitumor effects of combined anti-CD4-depleting antibody and anti-PD-1/PD-L1 immune checkpoint antibody treatment in mice. *Cancer Immunol Res* 3:631–640.
20. Lechner MG, et al. (2013) Immunogenicity of murine solid tumor models as a defining feature of in vivo behavior and response to immunotherapy. *J Immunother* 36: 477–489.
21. Chen L, et al. (1994) Tumor immunogenicity determines the effect of B7 costimulation on T cell-mediated tumor immunity. *J Exp Med* 179:523–532.
22. Murgueitio MS, et al. (2017) Enhanced immunostimulatory activity of in silico discovered agonists of Toll-like receptor 2 (TLR2). *Biochim Biophys Acta* 1861:2680–2689.
23. Guo X, et al. (2017) The novel toll-like receptor 2 agonist SUP3 enhances antigen presentation and T cell activation by dendritic cells. *Front Immunol* 8:158.
24. Guan Y, Omueti-Ayoade K, Mutha SK, Hergenrother PJ, Tapping RI (2010) Identification of novel synthetic toll-like receptor 2 agonists by high throughput screening. *J Biol Chem* 285:23755–23762.
25. Cheng K, et al. (2015) Specific activation of the TLR1-TLR2 heterodimer by small-molecule agonists. *Sci Adv* 1:e1400139.
26. Jin MS, et al. (2007) Crystal structure of the TLR1-TLR2 heterodimer induced by binding of a tri-acylated lipopeptide. *Cell* 130:1071–1082.
27. Freeman GJ, et al. (2000) Engagement of the PD-1 immunoinhibitory receptor by a novel B7 family member leads to negative regulation of lymphocyte activation. *J Exp Med* 192:1027–1034.
28. Nishimura H, Nose M, Hiai H, Minato N, Honjo T (1999) Development of lupus-like autoimmune diseases by disruption of the PD-1 gene encoding an ITIM motif-carrying immunoreceptor. *Immunity* 11:141–151.
29. Dong H, Zhu G, Tamada K, Chen L (1999) B7-H1, a third member of the B7 family, costimulates T-cell proliferation and interleukin-10 secretion. *Nat Med* 5:1365–1369.
30. Tang M, et al. (2015) Toll-like receptor 2 activation promotes tumor dendritic cell dysfunction by regulating IL-6 and IL-10 receptor signaling. *Cell Rep* 13:2851–2864.
31. Yamazaki S, et al. (2011) TLR2-dependent induction of IL-10 and Foxp3+ CD25+ CD4+ regulatory T cells prevents effective anti-tumor immunity induced by Pam2 lipopeptides in vivo. *PLoS One* 6:e18833.
32. Shime H, et al. (2017) Toll-like receptor 2 ligand and interferon-γ suppress anti-tumor T cell responses by enhancing the immunosuppressive activity of monocytic myeloid-derived suppressor cells. *Oncoimmunology* 7:e1373231.
33. Shen KY, et al. (2014) Molecular mechanisms of TLR2-mediated antigen cross-presentation in dendritic cells. *J Immunol* 192:4233–4241.
34. Nyirenda MH, et al. (2011) TLR2 stimulation drives human naive and effector regulatory T cells into a Th17-like phenotype with reduced suppressive function. *J Immunol* 187:2278–2290.
35. Zhang Y, et al. (2011) TLR1/TLR2 agonist induces tumor regression by reciprocal modulation of effector and regulatory T cells. *J Immunol* 186:1963–1969.
36. Amiset L, et al. (2012) TLR2 ligation protects effector T cells from regulatory T-cell mediated suppression and repolarizes T helper responses following MVA-based cancer immunotherapy. *Oncoimmunology* 1:1271–1280.